

Chlorine Kinetic Isotope Effects on the Haloalkane Dehalogenase Reaction

Andrzej Lewandowicz,[†] Juliusz Rudziński,[†] Lisa Tronstad,[‡] Mikael Widersten,[‡]
Per Ryberg,[§] Olle Matsson,[§] and Piotr Paneth*,[†]

Department of Chemistry, Technical University of Lodz, Zeromskiego 116, 90-924 Lodz, Poland,
Department of Biochemistry, Biomedical Center, Uppsala University, S-751 23 Uppsala, Sweden,
Department of Chemistry, Uppsala University, S-751 21 Uppsala, Sweden

Received September 26, 2000. Revised Manuscript Received March 7, 2001

Abstract: We have found chlorine kinetic isotope effects on the dehalogenation catalyzed by haloalkane dehalogenase from *Xanthobacter autotrophicus* GJ10 to be 1.0045 ± 0.0004 for 1,2-dichloroethane and 1.0066 ± 0.0004 for 1-chlorobutane. The latter isotope effect approaches the intrinsic chlorine kinetic isotope effect for the dehalogenation step. The intrinsic isotope effect has been modeled using semiempirical and DFT theory levels using the ONIOM QM/QM scheme. Our results indicate that the dehalogenation step is reversible; the overall irreversibility of the enzyme-catalyzed reaction is brought about by a step following the dehalogenation.

Introduction

In recent years, mechanisms of action of various dehalogenases have become a subject of intensive study¹ as a result of their potential use in bioremediation,² because halogenated organic compounds constitute the largest group of pollutants. Most of these enzymes react through formation of a covalently bonded intermediate, which is subsequently hydrolyzed to product,^{1p} although a direct displacement by a water molecule activated by an enzyme base has recently been reported.^{1c}

The reaction that is catalyzed by haloalkane dehalogenase from *Xanthobacter autotrophicus* GJ10 has been studied extensively.³ This enzyme catalyzes hydrolysis of the C–Cl bond of a carcinogenic pollutant, 1,2-dichloroethane [(ClCH₂)₂]. It was concluded that the first chemical step (top reaction in

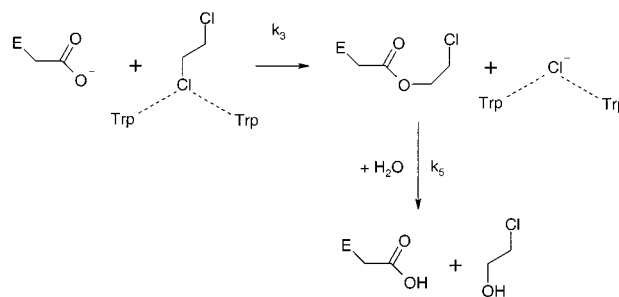


Figure 1. Chemical steps catalyzed by haloalkane dehalogenase.

Figure 1) is an S_N2 reaction, in which the chlorine atom is displaced by one of the carboxylic oxygens of the aspartate (Asp124) residue. This dehalogenation step, which leads to the enzyme-bounded intermediate, is believed to be irreversible. In the following reactions, abbreviated in Figure 1 to a single step, this intermediate is hydrolyzed by the nearby water molecule to the product. The chloride ion is hydrogen-bonded to two

[†] Technical University of Lodz.

[‡] Department of Biochemistry, Biomedical Center, Uppsala University.

[§] Department of Chemistry, Uppsala University.

(1) (a) Liu, J.-Q.; Kurihara, T.; Ichihara, S.; Miyagi, M.; Tsunasawa, S.; Kawasaki, H.; Soda, K.; Esaki, N. *J. Biol. Chem.* **1998**, *273*, 30897. (b) Nardi-Dei, V.; Koshikawa, H.; Esaki, N.; Sola, K. *Appl. Environ. Microbiol.* **1994**, *60*, 2389. (c) Zheng, Y.-J.; Bruice, T. C. *J. Am. Chem. Soc.* **1997**, *119*, 3868. (d) Nardi-Dei, V.; Kurihara, T.; Park, Ch.; Miyagi, M.; Tsunasawa, S.; Soda, K.; Esaki, N. *J. Biol. Chem.* **1999**, *274*, 20977. (e) Xiang, H.; Dong, J.; Carey, P. R.; Dunaway-Mariano, D. *Biochemistry* **1999**, *38*, 4207. (f) Dong, J.; Xiang, H.; Luo, L.; Dunaway-Mariano, D.; Carey, P. R. *Biochemistry* **1999**, *38*, 4198. (g) Taylor, K. L.; Xiang, H.; Liu, R.-Q.; Yang, G.; Dunaway-Mariano, D. *Biochemistry* **1997**, *36*, 1349. (h) Clarkson, J.; Tonge, P. J.; Taylor, K. L.; Dunaway-Mariano, D.; Carey, P. R. *Biochemistry* **1997**, *36*, 10192. (i) Benning, M. M.; Taylor, K. L.; Liu, R.-Q.; Yang, G.; Xiang, H.; Wesenberg, G.; Dunaway-Mariano, D.; Holden, H. M. *Biochemistry* **1996**, *35*, 8103. (j) Yang, G.; Liu, R.-Q.; Taylor, K. L.; Xiang, H.; Price, J.; Dunaway-Mariano, D. *Biochemistry* **1996**, *35*, 10879. (k) McCarthy, D. L.; Louie, D. F.; Copley, S. D. *J. Am. Chem. Soc.* **1997**, *119*, 11337. (l) McCarthy, D. L.; Navarrete, S.; Willett, W. S.; Babbitt, P. C.; Copley, S. D. *Biochemistry* **1996**, *35*, 14634. (m) Ordaz, E.; Garrido-Pertierra, A.; Gallego, M.; Puyet, A. *Biotechnol. Prog.* **2000**, *16*, 283. (n) Kunishima, M.; Friedman, J. E.; Rokita, S. E. *J. Am. Chem. Soc.* **1999**, *121*, 4722. (o) Anandarajah, K.; Kiefer, P. M., Jr.; Donohoe, B. S.; Copley, S. D. *Biochemistry* **2000**, *39*, 5303. (p) Verschuere, K. H. G.; Seljée, F.; Rozeboom, H. J.; Kalk, K. H.; Janssen, D. B.; Dijkstra, B. W. *Nature* **1993**, *363*, 693.

(2) (a) Wischnak, C.; Muller, R. *Biotechnology*, 2nd ed.; J. Wiley–VCH Verlag GmbH: Weinheim, Germany, 2000, 11b, pp 241. (b) Ridder, I. S.; Dijkstra, B. W. *CATTECH* **2000**, *3*, 126. (c) Chaudry, G. R.; Chapaladugu, S. *Microbiol. Rev.* **1991**, *55*, 59. (d) Fetzner, S.; Lingens, F. *Microbiol. Rev.* **1994**, *58*, 641.

(3) (a) Pikkemaat, M. G.; Ridder, I. S.; Rozeboom, H. J.; Kalk, K. H.; Dijkstra, B. W.; Janssen, D. B. *Biochemistry* **1999**, *38*, 12052. (b) Nardi-Dei, V.; Kurihara, T.; Park, Ch.; Miyagi, M.; Tsunasawa, S.; Soda, K.; Esaki, N. *J. Biol. Chem.* **1999**, *274*, 20977. (c) Verschuere, K. H. G.; Kingma, J.; Rozeboom, H. J.; Kalk, K. H.; Janssen, D. B.; Dijkstra, B. W.; *Biochemistry* **1993**, *32*, 9031. (d) Schanstra, J. P.; Ridder, I. S.; Heimeriks, G. J.; Rink, R.; Poelarends, G. J.; Kalk, K. H.; Dijkstra, B. W.; Janssen, D. B. *Biochemistry* **1996**, *35*, 13186. (e) Damborský, J.; Kutý, M.; Němec, M.; Koča, J. *J. Chem. Inf. Comput. Sci.* **1997**, *37*, 562. (f) Newman, J.; Peat, T. S.; Richard, R.; Kan, L.; Swanson, P. F.; Affholter, J. A.; Holmes, I. H.; Schindler, J. F.; Unkefer, C. J.; Terwilliger, T. C. *Biochemistry* **1999**, *38*, 16105. (g) Lightstone, F. C.; Zheng, Y.-J.; Bruice, T. C. *J. Am. Chem. Soc.* **1998**, *120*, 5611. (h) Lightstone, F. C.; Zheng, Y.-J.; Maulitz, A. H.; Bruice, T. *Proc. Natl. Acad. Sci. U.S.A.* **1997**, *94*, 8417. (i) Damborský, J.; Kutý, M.; Němec, M.; Koča, J. *J. Chem. Inf. Comput. Sci.* **1998**, *38*, 736. (j) Schanstra, J. P.; Janssen, D. B. *Biochemistry* **1996**, *35*, 5624. (k) Dijkstra, J. P.; Kingma, J.; Janssen, D. B. *J. Biol. Chem.* **1996**, *271*, 14747. (l) Schindler, J. F.; Naranjo, P. A.; Honaberger, D. A.; Chang, C.-H.; Brainard, J. R.; Vanderberg, L. A.; Unkefer, C. J. *Biochemistry* **1999**, *38*, 5772. (m) Robert, D.; Gironés, X.; Dorca, R. C. *J. Chem. Inf. Comput. Sci.* **2000**, *40*, 839. (n) Krooshof, G. H.; Ridder, I. S.; Tepper, A. W. J. W.; Vos, G. J.; Rozeboom, H. J.; Kalk, K. H.; Dijkstra, B. W.; Janssen, D. B. *Biochemistry* **1998**, *37*, 15013. (o) Widersten, M. *Protein Express. Purif.* **1998**, *13*, 389. (p) Krooshof, G. H.; Kwant, E. M.; Damborský, J.; Koča, J.; Janssen, D. B. *Biochemistry* **1997**, *36*, 9571.

tryptophan residues (Trp125 and Trp175), and its release from the enzyme determines the overall reaction rate.^{3c,k}

Because the rate-determining step occurs after the chemistry is accomplished, the details of the dehalogenation step are not amenable to direct kinetic scrutiny either under steady state or presteady-state conditions. Kinetic isotope effects provide powerful insight into details of chemical and enzymatic reactions.⁴ We have taken advantage of the fact that under competitive conditions, kinetic isotope effects provide information about steps through the first irreversible step to shed some light on the nature of the dehalogenation step.

We present here experimental and theoretical studies of chlorine kinetic isotope effects on the haloalkane dehalogenase reaction. We have compared isotope effects for the “natural” substrate, 1,2-dichloroethane and the “slow substrate”, 1-chlorobutane. In the reaction course the enzyme-bound reactant (ES) is converted to a covalently bound intermediate (EI), which can either react or return the substrate to the solution. We argue that if the reaction toward products were irreversible, then there should be no difference between the heavy-atom isotope effects measured for 1,2-dichloroethane and 1-chlorobutane. If, however, EI can bounce back to ES and then go forward again, the heavy-atom isotope effect should be attenuated. We have found chlorine isotope effects of 1.0045 for 1,2-dichloroethane, as compared with a value of 1.0066 for 1-chlorobutane. This significant difference is taken to imply that the reverse reaction of EI is not zero. We present a quantitative computational model to account for this interpretation.

Experimental Section

Materials. The highest commercial grades of 1,2-dichloroethane, and mercuric (II) thiocyanate from Sigma; nitric acid and silver nitride from POChem (Gliwice, Poland); 1-chlorobutane (ⁿBuCl) from Fluka; 1,3-bis[tris-(hydroxymethyl)methylamino]propane (bis-tris-propane, BTP) from CALBIOCHEM; and ferric ammonium sulfate (Technabexport, Soviet Union) were used without further purification. Haloalkane dehalogenase (EC 3.8.1.5) from *X. autotrophicus* GJ10 was obtained as described earlier.^{3o}

Isotope Effect Measurements. 1,2-dichloroethane (final concentration, 25 mM) or 1-chlorobutane (final concentration, 6.7 mM) was dissolved in 10 mL of chloride-free 50 mM bis-tris-propane buffer, pH 7.3 at 34 °C. The reaction was started by addition of 0.66 unit of haloalkane dehalogenase (concentration, 0.7 mg/mL; activity, 3.3 u/ml). Reaction progress was determined by monitoring chloride concentration using a standard colorimetric assay⁵ at 460 nm.

Reaction mixtures for small conversion analysis were quenched at the desired fractions of reaction (5–30%) with concentrated nitric acid. Reaction mixtures for the analysis of full conversion were left for 24 h and then quenched. Chloride was then precipitated with silver nitrate. The precipitate was centrifuged for 3 min at 5000 rotation/min then washed with 2 mL of water and centrifuged again. The washing procedure was repeated three times, and AgCl was left to dry over P₂O₅ in a vacuum desiccator in the dark. All of the measurements were repeated independently five times.

The isotopic ratios ³⁷Cl/³⁵Cl were measured by the FAB-IRMS technique developed in our laboratory,⁶ and the isotope effect was calculated from isotopic ratios of the reactant before reaction and the product after small conversion from the equation⁴

$${}^{37}k_{\text{obs}} = \frac{k_{35}}{k_{37}} = \frac{\ln(1-f)}{\ln(1-fR_p/R_0)} \quad (1)$$

where k_{35}/k_{37} is the chlorine kinetic isotope effect; f , the fraction of

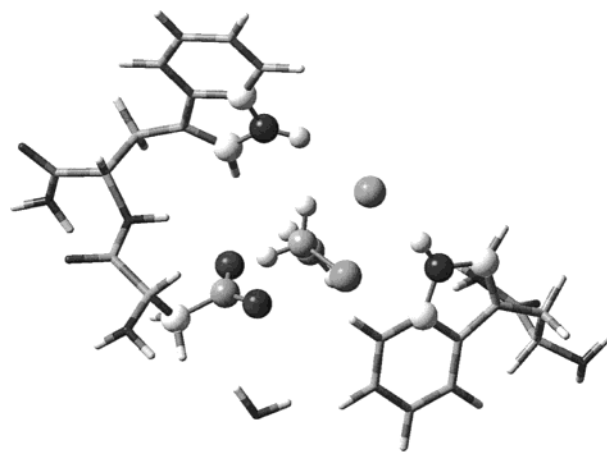


Figure 2. Model of the active site with the transition state for the dehalogenation step. See text for more details.

reaction; and R , the isotopic ratio of the reactant (0) or product (f). The first equation introduces the Northrop notation of isotope effects, which uses a leading superscript to indicate that the symbol corresponds to an isotope effect rather than a rate constant. The leading superscripts correspond to the heavy isotope that is used. The subscript that follows the variable is used to identify elementary reactions in the complex mechanism.

Computational Section. Two models of (ClCH₂)₂ in an aqueous environment were used. In the first model, two explicit water molecules were positioned at hydrogen bonding distance from one of the chlorine atoms, and the structure was optimized at the semiempirical and DFT levels. In the second model, the continuum COSMO model⁷ of solvent was used.

The model for the dehalogenation step in the active site of the enzyme was constructed on the basis of the crystal structure of the enzyme–chloride ion complex deposited in the Protein Data Bank (2DHC). It contains residues Asp124, Trp125, Trp175, one water molecule (water485), and either (ClCH₂)₂ or ⁿBuCl, which were manually docked into the active site. N-terminals were capped with hydrogens and C-terminals were capped with amino groups yielding 79-atom and 85-atom models for active sites with (ClCH₂)₂ or ⁿBuCl, respectively. Figure 2 illustrates the model that was used for the example of an optimized transition-state structure. Other features of Figure 2 are explained in the following sections.

In all cases, the transition state was identified by one imaginary frequency corresponding to transition from reactants to products (both having only real harmonic vibrational frequencies). Intrinsic chlorine kinetic isotope effects were calculated using the ISOEFF98 program⁸ from the complete equation.⁴

$${}^{37}k = \frac{k_{35}}{k_{37}} = \frac{v_{35}^{\ddagger}}{v_{37}^{\ddagger}} \times \prod_i \frac{u_{i35}^{\ddagger} \cdot \sinh(u_{i37}/2)}{u_{i37}^{\ddagger} \cdot \sinh(u_{i35}/2)} \times \prod_i \frac{u_{i37}^{\ddagger} \cdot \sinh(u_{i35}^{\ddagger}/2)}{u_{i35}^{\ddagger} \cdot \sinh(u_{i37}^{\ddagger}/2)} \quad (2)$$

where k_{35}/k_{37} is the kinetic isotope effect, n is the number of atoms, $u = hv/k_B T$ (where h and k_B are Planck and Boltzmann constants, respectively), T is the absolute temperature, and v_i is the frequencies of normal modes of vibrations. The superscript \ddagger indicates the properties of the transition state.

For calculations of the binding isotope effect, three modifications were introduced into eq 2. First, the ratio $v_{35}^{\ddagger}/v_{37}^{\ddagger}$ was omitted, because the equilibrium isotope effect was being calculated. Second, the first multiplication term extended over $3n_{\text{aq}}-6$ terms, where n_{aq} is the number of atoms in the model of (ClCH₂)₂ in aqueous solution. Third, the second multiplication term extended over $3n-6$ terms and corresponded to the model of the reactant bounded in the active site.

(6) Westaway, K. C.; Koerner, T.; Fang, Y.-R.; Rudziński, J.; Paneth, P. *Anal. Chem.* **1998**, *70*, 3548.

(7) Klamt, A.; Schüürmann, G. *J. Chem. Soc., Perkin Trans. 2* **1993**, 799.

(8) Anisimov, V.; Paneth, P. *J. Math. Chem.* **1999**, *26*, 75.

(4) Melander, L.; Saunders, W. H., Jr. *Reaction Rates of Isotopic Molecules*; Wiley and Sons: New York, 1980.

(5) Iwasaki, I.; Utsumi, S.; Hagino, K.; Ozawa, T. *Bull. Chem. Soc. Jpn.* **1956**, *29*, 860.

Table 1. Theoretical Chlorine Kinetic Isotope Effects on the Dehalogenation Step and Model Reactions

theory level	Trp models ^a	ⁿ BuCl	(CH ₂ Cl) ₂
B1LYP/6-31G*		1.00738 ^b	1.00802 ^c
B1LYP/6-31G*:AM1	NH ₃		1.00696
B1LYP/6-31G*:PM3	NH ₃	1.00634	1.00649 (1.00634) ^d
	pyrrole rings	1.00613	1.00629
	indole rings	1.00650	
B1LYP/6-31+G*:PM3	NH ₃		1.00680

^a Part of the tryptophans included in the high level of the QM/QM calculations (see text). ^b Reaction with MeO⁻ in methanol modeled using COSMO continuum solvent model. ^c Gas-phase reaction with HCO₂⁻. ^d Obtained using scaled frequencies (see text).

Semiempirical Calculations. AM1⁹ and PM3¹⁰ Hamiltonians as implemented in HyperChem 5.1 (Hypercube, Inc., FL) were used. To obtain approximate geometry, a simple transition state of the S_N2 reaction in the gas phase between (ClCH₂)₂ and free Asp was modeled using the Quadratic Synchronous Transit method. The structure thus obtained was then inserted into the active site cavity model, ensuring that the departing chloride was placed between hydrogens of indole rings of Trp125 and Trp175, and the Eigenvector Following method was used to find the geometry of the new transition state. The models for the ⁿBuCl reaction were obtained by changing (ClCH₂)₂ into ⁿBuCl, followed by reoptimization.

QM/QM Calculations. Structures of the reactant and transition state optimized at the semiempirical level were taken as initial structures for the QM/QM calculations. The ONIOM method¹¹ as implemented in the Gaussian package¹² was used. The model was divided into two layers. These are distinguished in Figure 2 by different rendering; the "higher" layer is presented by balls and sticks; for the "lower" layer, tubes are used. Five carbon link atoms were treated as hydrogens in the higher-level calculation. This model is labeled as NH₃ in Table 1 because both tryptophan residues are truncated to ammonia in the higher layer. For comparison, we have also calculated isotope effects for models in which pyrrole and indole rings were used as models for tryptophans. Optimization of geometries, followed by force field and isotope effect calculations, was performed at B1LYP/6-31G*:AM1, B1LYP/6-31G*:PM3, and B1LYP/6-31+G*:PM3 levels of theory. The B1LYP/6-31G*:PM3 level is regarded as the reference for other calculations. The B1LYP method was chosen because it was optimized to yield good quality vibrational frequencies.¹³ We have noticed a similar improvement over the B3LYP method in studies (Paneth et al., unpublished) of a model S_N2 reaction, although no significant changes in the resulting isotope effects were observed. For comparison, gas-phase calculations were also performed on a model comprising a (ClCH₂)₂ molecule and formate ion at the B1LYP/6-31G* level. Modeling of S_N2 mechanisms with DFT methods is well-documented in literature¹⁴ for reactions in both gas and condensed phases. We have further validated the use of the B1LYP/6-31G* level of theory by calculating the chlorine kinetic isotope effect for the reaction between ⁿBuCl and methoxide in methanol at 40 °C. The calculated value of 1.00738 is in excellent agreement with the experimentally¹⁵ determined $k_{35}/k_{37} = 1.0074$. Although the applicability of the kinetic model described here to gas-phase nucleophilic displacement might be

questioned,¹⁶ the good fit to the data in ref 15 tests the appropriateness of the model to solution.

Results

Experimentally, the chlorine kinetic isotope effect on the dehalogenation of 1,2-dichloroethane catalyzed by haloalkane dehalogenase from *X. autotrophicus* GJ10 has been found to be 1.0045 ± 0.0004 . The chlorine kinetic isotope effect for 1-chlorobutane, a slow substrate of haloalkane dehalogenase with $k_{\text{cat}}/K_M \sim 160$ times smaller than that for 1,2-dichloroethane, has been found to be 1.0066 ± 0.0004 .

Calculated values of the intrinsic chlorine kinetic isotope effects are collected in Table 1. For the reference level, calculations without scaling of frequencies as well as with using a scaling factor¹⁷ of 0.9806 were performed. The isotope effect calculated with scaling is reported in parentheses. In agreement with our earlier findings,¹⁸ scaling of frequencies has a negligible effect on the isotope effect. For all other calculations, unscaled harmonic vibrational frequencies were used.

In calculations of anionic species, it is usually important to include diffuse orbitals. We have compared calculations performed at 6-31G* and 6-31+G* levels and found negligible change of the resulting geometries and the isotope effect. For the reference level of calculations (B1LYP/6-31G*:PM3), the activation barrier was found to be 15.7 kcal/mol and the exothermicity, 13.7 kcal/mol. The corresponding values for the model including (ClCH₂)₂ and formate using B1LYP/6-31G* calculations in the gas-phase resulted in 13.8 and 9.7 kcal/mol for the activation barrier and the heat of reaction, respectively. Surprisingly, the inclusion of diffuse orbitals increases the activation energy to 19.3 kcal/mol. Calculations using different models of the tryptophan residues yielded essentially the same results.

Basic geometric properties of the transition state, calculated at different theory levels, are listed in Table 2. In this table, changes of the appropriate parameters upon transition from the reactant to the transition state are given in parentheses, except for the forming O–C bond, where the change in the parentheses indicates the difference between the transition state and the product. The positive value of the change corresponds to the increase of a given parameter.

The kinetic isotope effect for the reverse direction of the dehalogenation step (elementary step with the rate constant k_4) was calculated using the same transition-state model and the product of the dehalogenation, enzyme-bound intermediate. At the reference level, this isotope effect was found to be 1.0004. The equilibrium isotope effect on the binding of (ClCH₂)₂ by haloalkane dehalogenase was found to be 0.9994 for the continuum COSMO model and 1.0003 for the model that included two explicit water molecules hydrogen-bonded to the chlorine atom.

The C–Cl bond length in the transition state is equal to 2.20 Å for PM3 (increase of 0.41 Å over the reactant) and 2.21 Å for AM1 (increase of 0.54 Å). The bond length of the forming

(9) Dewar, M. J. S.; Zebisch, E. G.; Healy, E. F.; Stewart, J. J. P. *J. Am. Chem. Soc.* **1985**, *107*, 3902.

(10) Stewart, J. J. P. *J. Comput. Chem.* **1989**, *10*, 209, 221.

(11) Maseras, F.; Morokuma, K. *J. Comput. Chem.* **1995**, *16*, 1170.

(12) Frisch, M. J.; Trucks, G. W.; Schlegel, H. B.; G. E. Scuseria; Robb, M. A.; Cheeseman, J. R.; Zakrzewski, V. G.; J. A. Montgomery, J.; Stratmann, R. E.; Burant, J. C.; Dapprich, S.; Millam, J. M.; Daniels, A. D.; Kudin, K. N.; Strain, M. C.; Farkas, O.; J. Tomasi; Barone, V.; Cossi, M.; Cammi, R.; Mennucci, B.; Pomelli, C.; C. Adamo; Clifford, S.; Ochterski, J.; Petersson, G. A.; Ayala, P. Y.; Cui, Q.; Morokuma, K.; Malick, D. K.; Rabuck, A. D.; K. Raghavachari; Foresman, J. B.; Cioslowski, J.; Ortiz, J. V.; Stefanov, B. B.; G. Liu; Liashenko, A.; Piskorz, P.; Komaromi, I.; Gomperts, R.; R. L. Martin; Fox, D. J.; Keith, T.; Al-Laham, M. A.; Peng, C. Y.; A. Nanayakkara; Gonzalez, C.; Challacombe, M.; Gill, P. M. W.; Johnson, B.; W. Chen; Wong, M. W.; Andres, J. L.; Gonzalez, C.; Head-Gordon, M.; Replogle, E. S.; Pople, J. A. *Gaussian 98*; A.9

(13) Becke, D. A. *J. Chem. Phys.* **1996**, *104*, 1040.

(14) (a) Safi, B.; Choho, K.; Geerlings, P. *J. Phys. Chem. A* **2001**, *105*, 591. (b) Shaik, S. S.; Schlegel, H. B.; Wolfe, S. *Theoretical Aspects of Physical Organic Chemistry. The S_N2 Mechanism*; John Wiley: New York, 1992. (c) Kreevoy, M. M.; Truhlar, G. G. In *Investigation of Rates and Mechanisms of Reactions*; Bernasconi, F. C., Ed.; Techniques of Chemistry Series; John Wiley: New York, 1986; Vol. IV. (d) Knoerr, E. H.; Eberhart, M. E. *J. Phys. Chem. A* **2001**, *105*, 880. (e) Lynch, B. J.; Fast, P. L.; Harris, M.; Truhlar, D. G. *J. Phys. Chem. A* **2000**, *104*, 4811.

(15) Grimrod, E. P.; Taylor, J. W. *J. Am. Chem. Soc.* **1970**, *92*, 739.

(16) (a) Schmatz, S. *Chem. Phys. Lett.* **2000**, *330*, 188. (b) Tonner, D. S.; McMahon, T. B. *J. Am. Chem. Soc.* **2000**, *122*, 8783.

(17) Scott, A. F.; Radom, L. *J. Phys. Chem.* **1996**, *100*, 16502.

(18) Paneth, P. *Comput. Chem.* **1995**, *19*, 11.

Table 2. Optimized Basic Geometric Parameters for the Transition State of the Dehalogenation Step^a

theory level	C···Cl	O···Ca ^b	Cl···HN	NH···Cl	O···C···Cl	H···Cl···H
B1LYP/6-31G*:AM1	2.37 (0.53)	2.10 (0.64)	2.40 (-0.16)	2.30 (-1.22)	164.5 (3.7)	128.3 (15.7)
B1LYP/6-31G	2.31 (0.52)	2.10 (0.64)			164.5 (-)	
B1LYP/6-31G*:PM3	2.35 (0.51)	2.09 (0.64)	2.46 (-0.32)	2.40 (-0.35)	166.5 (3.4)	151.2 (5.0)
B1LYP/6-31+G*:PM3	2.38 (0.55)	2.08 (0.62)	2.47 (-0.33)	2.39 (-0.42)	165.9 (8.0)	144.9 (3.7)

^a Bond distances and their changes are given in Å, angles in degrees. Changes from values for the reactant are given in parentheses ^b Changes from the product geometry are reported for the C–O bond.

O–C bond is 1.98 and 1.93 Å for PM3 and AM1, respectively. When compared to the reference level, both semiempirical methods overestimate (data not shown) the covalent character of the C–Cl bond retained in the transition state. Our results obtained at the reference level are in very good agreement with those obtained earlier at the Hartree–Fock level.^{3g} Geometries of the reactant in the active site obtained using the AM1 method (AM1 and B1LYP/6-31G*:AM1 levels) yielded unrealistic geometries. In the case of AM1 calculations, both of the chlorine atoms of (ClCH₂)₂ are hydrogen-bonded to tryptophans, but in the case of B1LYP/6-31G*:AM1, the model folded, thus placing two tryptophans in a stacked position. Notably, the isotope effect calculated on the basis of these geometries is reasonable. This indicates that changes in the force constants of stretching modes are the major contributors to the isotope effect.

Discussion

Modeling of the Intrinsic Isotope Effect. Because enzymatic reactions involve large numbers of atoms, the use of semiempirical methods seems mandatory. To draw mechanistic conclusions from isotope effects, however, it is of importance to have a method that reliably predicts geometries and isotope effects. Two semiempirical parametrizations, AM1 and PM3, have been used previously in the modeling of the dehalogenation catalyzed by the haloalkane dehalogenase. Bruice and co-workers have argued for the PM3 parametrization, because the resulting geometrical parameters of the transition state are very close to those obtained for small models using the HF/6-31+G(d) basis set and because the AM1 method gives bifurcated hydrogen bonds and a large error in the heat of formation of the chlorine atom.^{3h} Damborský et al.,^{3e} on the other hand, favor the AM1 Hamiltonian, citing its suitability for S_N2 reactions, agreement between results obtained by this method and DFT/6-31G**, its ability to correctly reproduce the activation energy of the reaction between Cl⁻ and CH₃Cl, geometries of hydrogen bonds, and excellent energetic results in the studies of the carboxypeptidase mechanism. Our own experience with the modeling of chlorine kinetic isotope effects indicates that the PM3 method underestimates these effects. Furthermore, for a model S_N2 reaction (to be published elsewhere), when compared to the high-level ab initio calculations, both of these methods substantially underestimate the extent of the C–Cl bond cleavage in the transition state. This suggests that semiempirical methods alone are not capable of reliable prediction of chlorine kinetic isotope effects.

The theoretical intrinsic isotope effect from our QM/QM calculations is about 1.0065 (for the reference B1LYP/6-31G*:PM3 level), and corresponds to the observed isotope effect for the slow substrate ¹²⁵BuCl. The approach of the nucleophile deviates from collinearity with the breaking C–Cl bond by about 14°. This is probably caused by the steric hindrance of the carboxylate approach, which drags tryptophan rings from their optimal positions. The breaking C–Cl bond is elongated by about 0.5 Å as compared to the length of this bond in the reactant, and the forming O–C bond is longer than the one in

the product of the dehalogenation step by 0.64 Å. These changes can be used to estimate bond orders using the Pauling rule. The formal bond orders in the transition state are 0.18 and 0.12 for C–Cl and O–C bonds, respectively. In the traditional, qualitative description of transition states, this corresponds to the symmetrical, exploded (loose) transition state.

Our long-term goal is to model the whole haloalkane dehalogenase catalyzed reaction. To achieve this goal, however, a much larger model of the enzyme is necessary. A minimal model that includes all of the residues known to be of importance in the overall reaction contains nearly 500 atoms. Ab initio levels are impractical for such large systems. Recently developed QM/MM techniques, which offer reasonable compromise between computational efficiency and precision, have been successfully applied in studies of enzyme-catalyzed reactions.¹⁹ Our ONIOM model used for the dehalogenation step can be readily upgraded to this level by including an MM layer around it. Thus, the model used here allows critical evaluation of the semiempirical methods, reliably predicts the intrinsic isotope effect, and can be used in studies of the mechanisms of all of the steps of the haloalkane dehalogenase reaction.

Dehalogenase Mechanism. We start our discussion with the observation that the experimental isotope effect for the “natural” substrate, (ClCH₂)₂, is quite small. Typically, chloride-leaving-group kinetic isotope effects²⁰ for S_N2 reactions are in the range of 1.0057–1.0095. The small value of the observed isotope effect may result from a small intrinsic isotope effect or from the reaction complexity. To distinguish between these two possibilities, we have measured the isotope effect for the ¹²⁵BuCl reaction. The *k*_{cat}/*K*_M for ¹²⁵BuCl is 2 orders of magnitude smaller,³¹ and thus, the measured isotope effect should be very close to the intrinsic value. The observed substantial increase of the observed value of the isotope effect rules out the possibility of a small intrinsic isotope effect.

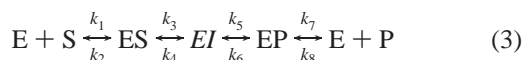
At this point, we feel it is necessary to comment on the magnitude of the isotope effects that are discussed here. Both measured isotope effects are small in the absolute sense. It is much easier to think of these (and other heavy-atom) isotope effects in terms of deviation from unity, usually expressed in terms of a percent. In this terminology, the values measured by us for (ClCH₂)₂ and ¹²⁵BuCl are 0.45 and 0.66%, respectively,

(19) (a) Várnai, P.; Richards, W. G.; Lyne, P. D. *Proteins: Struct., Funct., Genet.* **1999**, *37*, 218. (b) Mulholland, A. J.; Richards, W. G. *Proteins: Struct., Funct., Genet.* **1997**, *27*, 9. (c) Alhambra, C.; Gao, J.; Corchado, C. J.; Villá J.; Truhlar, D. G. *J. Am. Chem. Soc.* **1999**, *121*, 1, 2253. (d) Alhambra, C.; Gao, J. *J. Comput. Chem.* **2000**, *21*, 1192. (e) Greatbanks, S. P.; Gready, J. E.; Limaye, A. C.; Kendell, A. P. *Proteins: Struct., Funct., Genet.* **1999**, *37*, 157. (f) Himo, F.; Eriksson, L. A.; Maseras, F.; Siegbahn, P. E. M. *J. Am. Chem. Soc.* **2000**, *122*, 8031. (g) Pawlak, J.; O’Leary, M. H.; Paneth, P. *ACS Symp. Ser.* **1999**, *721*, 462. (h) Ridder, L.; Mulholland, A. J.; Rietjens, I. M. C. M.; Vervoort, J. *J. Am. Chem. Soc.* **2000**, *122*, 8728. (i) Cummins, P. L.; Gready, J. E. *J. Comput. Chem.* **1990**, *11*, 791. (j) Cummins, P. L.; Gready, J. E. *J. Comput. Chem.* **1998**, *19*, 977. (k) Zhang, Y.; Liu, H.; Yang, W. *J. Chem. Phys.* **2000**, *112*, 3483. (l) Cui, Q.; Karplus, M. *J. Chem. Phys.* **2000**, *112*, 1133.

(20) Shiner, V. J., Jr.; Wilgis, F. P. In *Isotopes in Organic Chemistry*; Buncl, E., Saunders, W. H., Jr., Eds.; Elsevier: Amsterdam, 1992; Vol. 8, 272.

on the scale of 0 to ~1%, observed for chlorine isotope effects.²⁰ The isotope effect for ¹⁰⁹BuCl is, thus, larger than the one for (ClCH₂)₂ by about half of its value! Contemporary experimental techniques ensure precision, which allows confident determination of these differences. We can, therefore, confidently state that observed chlorine kinetic isotope effects indicate that the reaction complexity partially masks the intrinsic value in the case of the (ClCH₂)₂.

We will now consider the overall reaction equation and its correlation with the observed isotope effects. Eq 3 illustrates a reaction sequence that describes most of the features of the enzymatic process in question. According to this equation, in the first step, the reactant is binding to the enzyme, forming the Michaelis complex, which in the subsequent step reacts to form the enzyme-bound intermediate EI and a chloride ion. The EI complex is then hydrolyzed to the final product 2-chloroethanol in a reaction characterized by the forward rate constant, *k*₅. The product is released from the enzyme in the final step. Kinetic data indicate that the release of the chloride ion from the enzyme is the rate-determining step.



Although the steady-state and presteady-state kinetic studies do not indicate any additional steps preceding the dehalogenation, the presence of isotope insensitive step(s), for example, conformational changes of the enzyme preceding the dehalogenation is possible. For the sake of simplicity, these steps are not shown and, therefore, are included in the first step of eq 3.

The overall reaction is irreversible,^{3j,k} and it is assumed that the dehalogenation step is irreversible, for example, the rate constant *k*₄ is practically equal to zero. In the following discussion, we will argue that this assumption does not agree with the chlorine fractionation pattern reported herein.

Under competitive conditions, kinetic isotope effects provide information about steps through the first irreversible step. Equation 4 correlates the observed isotope effect with the intrinsic one (the isotope effect on *k*₃, the dehalogenation step);

$${}^{37}k_{\text{obs}} = \frac{{}^{37}k_3 + c}{1 + c} \quad (4)$$

c is called the forward commitment,²¹ and for this particular case, is equal to *k*₃/*k*₂.

Equation 4 has been derived under the assumption that there are no chlorine isotope effects on steps preceding dehalogenation, which in this case includes binding and possible conformational changes. We have shown previously that binding may give rise to measurable isotope effects, even in the case of heavy atoms.²² For the present case, however, isotope effects calculated for the equilibrium between the reactant in solution (continuum models as well as explicit solvation by two water molecules, data not shown) and the reactant in the active site are negligible. Conformational changes are not expected to yield substantial isotope effects, either.

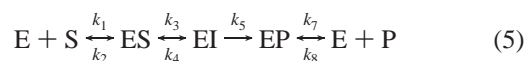
Assuming that the value obtained for ¹⁰⁹BuCl is equal to the intrinsic isotope effect (assumption supported by the results of calculations), we can calculate *c* ≈ 0.5. On the basis of the best fit of kinetic data, Janssen^{3k} evaluated the individual rate

constants. These data lead to a forward commitment, *c*_f, for the overall reaction of ~2.5. Because the dehalogenation step is supposed to be the first irreversible step, the two commitments (*c* and *c*_f) should be equal. The value derived from the analysis of the isotope effect, however, differs significantly from *c*_f resulting from kinetic fitting. Although parameters obtained by fitting data can bear substantial error, the discrepancy between these two estimates of the commitment is too large to be accounted for by experimental error.

Alternatively, it can be assumed that the commitment based on kinetic data-fitting is correct (*c* = *c*_f ~ 2.5) for the (ClCH₂)₂ reaction. This assumption, however, requires the intrinsic isotope effect to be >1.0158. This value is much larger than any reported chlorine isotope effect.²⁰ Furthermore, it disagrees with the results of modeling of the intrinsic isotope effect presented herein (see Table 1) as well as in other model studies (Paneth et al., unpublished).

Finally, one can assume that the intrinsic value is different for the two reactants. We have shown earlier, however, that although one can expect small deviations of the intrinsic isotope effects^{19g} depending on the nature of substrate, the changes are expected to be an order of magnitude smaller than the observed differences in isotope effects for (ClCH₂)₂ and ¹⁰⁹BuCl. In addition, our results of modeling isotope effects for these two reactants support the idea that the intrinsic values for both of them should be similar (see Table 1); thus, we conclude that the experimental isotope effects reported herein cannot be satisfactorily explained within the proposed model in which the dehalogenation step is irreversible.

To find an explanation consistent with all of the experimental evidence, one has to turn to reaction schemes for which the forward commitment differs from the commitment for the chlorine isotope effect. The simplest examples are reactions with reversible isotope-sensitive steps. Let us consider again the general reaction equation (3), but this time, assuming *k*₆ to be equal to zero.



The forward commitment for this reaction equals *c*_f = *k*₅/*k*₄(1 + *k*₃/*k*₂), and the observed isotope effect is correlated with the intrinsic isotope effect by the equation

$${}^{37}k_{\text{obs}} = \frac{{}^{37}k_3 + \frac{c_f - k_5/k_4}{1 + k_5/k_4}}{1 + \frac{c_f - k_5/k_4}{1 + k_5/k_4}} \quad (6)$$

In addition to assumptions made for eq 4 in deriving eq 6, it has been assumed that the elementary reaction reverse dehalogenation (*k*₄) does not exhibit a sizable chlorine isotope effect. There are two factors governing the magnitude of heavy-atom isotope effects. One originates in the mass difference, and it always favors the light species. The other reflects the tightness of bonding around the isotopic atom, with heavy species concentrating in tighter surroundings. Thus, in a process of breaking a bond to the isotopic atom (like the dehalogenation forward reaction, *k*₃) both factors favor the light species, and the resulting isotope effect is large. In a process in which a new bond is being formed to the isotopic atom (like the reverse reaction, *k*₄, of the dehalogenation step), these factors act in opposite directions, mostly canceling each other and leading to a very small or no isotope effect. In agreement with this

(21) (a) Cook, P. F.; Cleland W. W. *Biochemistry* **1981**, *20*, 1790. (b) Hermes, J. D.; Roeske, C. A.; O'Leary, M. H.; Cleland W. W. *Biochemistry* **1982**, *21*, 5106.

(22) (a) Gawlita, E.; Anderson, V. E.; Paneth, P. *Biochemistry* **1995**, *34*, 6050. (b) Gawlita, E.; Anderson, V. E.; Paneth, P. *Eur. Biophys. J.* **1994**, *23*, 353. (c) Rakowski, K.; Paneth, P. *J. Mol. Struct.* **1996**, *378*, 35.

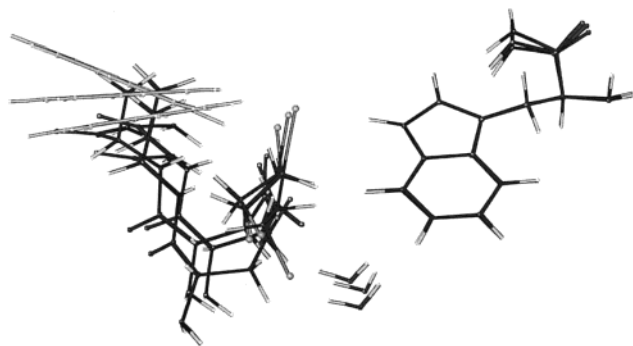


Figure 3. Overlay of stationary points of the dehalogenation step; reactants, ES (bottom), transition state (center), and product, EI (top). All structures are superimposed along the H–N bond of Trp175 with rings of Trp125 oriented perpendicularly to the plane and labeled in yellow.

reasoning, our calculation yielded a chlorine kinetic isotope effect for the reverse reaction $^{37}k_4 = 1.0004$ at the reference theory level.

Using values $^{37}k_{\text{obs}} = 1.0045$, $^{37}k_3 = 1.0066$, and $c_f = 2.5$, it is possible to calculate individual rate constant ratios: $k_5/k_4 = 1.4$ and $k_3/k_2 = 0.8$. Upon changing the reactant, the dehalogenation step becomes much slower, that is, k_3/k_2 approaches zero, c_f approaches k_5/k_4 , and consequently, $^{37}k_{\text{obs}}$ approaches $^{37}k_3$, as has been observed experimentally.

Further support for the proposed mechanism comes from the modeling of the reaction in the active site. In order for the carboxylic moiety of Asp124 to act as the nucleophile, it has to move $>1 \text{ \AA}$ toward the carbon atom of $(\text{ClCH}_2)_2$. This aspartate is directly connected to Trp125, which participates in the hydrogen bonding of the chlorine atom; thus, the optimal geometry for the hydrogen-bonding network has to be compromised to allow nucleophilic attack by the carboxyl group. As a result, the tryptophan rings are rotated out of their optimal positions during the reaction, as illustrated in Figure 3. Thus, the dehalogenation step “resembles” drawing a bow; the high-energy cost is compensated by the increased hydrogen bonding to the chlorine atom. The hydrolysis triggers release of the strain and return of the tryptophan residue to the optimal position. The reverse process is energetically unfavorable.

Irreversibility of the dehalogenation step was supported by the energetic profile of the overall reaction that was derived from the AM1 calculations.³¹ In this profile, an activation energy

of 25 kcal/mol for the dehalogenation step has been assumed. These same authors, however, reported a value of 21 kcal/mol in the preceding paper.^{3e} Semiempirical methods are known to overestimate energetic barriers, and furthermore, in the methodology employed, structures of the transition state were not reoptimized. Lowering the activation barrier for the dehalogenation step to ~ 15 kcal/mol would, in fact, change the energetics of the reaction consistent with our hypothesis. It would also agree with the calculated value of ~ 1.4 for the k_5/k_4 ratio. The activation energy of 15.7 kcal/mol that was obtained in our studies fits reasonably well with this picture. DFT methods, however, tend to underestimate energetic barriers; thus, this barrier cannot be compared directly with the activation energy of the subsequent step that is derived from semiempirical calculations. Clearly, modeling of all steps of the dehalogenase reaction at a level more reliable than semiempirical is needed to fully test the hypothesis proposed here. Such studies are underway in this and other laboratories (Gao et al., personal communication).

Conclusions

We have measured chlorine kinetic isotope effects on the reaction that is catalyzed by the haloalkane dehalogenase. The experimental values were found to be 0.45% for $(\text{ClCH}_2)_2$ and 0.66% for $^n\text{BuCl}$. Both semiempirical and DFT calculations indicate that the latter value corresponds to the intrinsic isotope effect. Analysis of the chlorine fractionation pattern, together with known kinetic data, leads to the conclusion that the dehalogenation step is reversible and the overall irreversibility of the haloalkane dehalogenase-catalyzed reaction is caused by the following step, hydrolysis of the enzyme-bound intermediate.

Acknowledgment. Support from the State Committee for Scientific Research (KBN, Poland), the Joint Polish-American Maria Skłodowska-Curie Fund II (P.P.), the Swedish Natural Science Research Council (O.M.), and the Swedish Research Council for Engineering Sciences and the Carl Trygger Foundation (M.W.) are gratefully acknowledged. P.P. acknowledges Fulbright and Swedish Institute scholarships. Computer time at the Polish Supercomputer Centers in Cracow, Warsaw, and Poznan, and the Minnesota Supercomputer Institute are acknowledged.

JA003503D